

## Low-temperature specific heat of single-wall carbon nanotubes

J. C. Lasjaunias,<sup>1,\*</sup> K. Biljaković,<sup>1,2</sup> Z. Benes,<sup>3</sup> J. E. Fischer,<sup>3</sup> and P. Monceau<sup>1</sup>

<sup>1</sup>*CRTBT-CNRS, BP 166, 38042 Grenoble Cedex 9, France*

<sup>2</sup>*Institute of Physics, P.O.B. 304, HR-10001 Zagreb, Croatia*

<sup>3</sup>*University of Pennsylvania, Philadelphia, Pennsylvania 19104-6272*

(Received 21 September 2001; published 22 February 2002)

Previous low-temperature heat capacity measurements down to 2 K have been analyzed as resulting from one-dimensional quantum confinement of single-wall carbon nanotube (SWNT) vibrational modes [J. Hone *et al.*, *Science* **289**, 1730 (2000)]. We extended the measurements on SWNT ropes from the same preparation technique down to 0.1 K. The specific heat shows three contributions: a well-defined  $T^{-2}$  term from nuclear hyperfine interactions in ferromagnetic impurities and a monotonously varying vibrational contribution very sensitive to adsorbed gases, in particular  $^4\text{He}$ . In the best outgassing conditions, the specific heat yields the  $T^3$  term originating from intertube coupling, in agreement with J. Hone *et al.* [*Science* **289**, 1730 (2000)]. The third contribution follows sublinear, power-law  $T$  dependence. We discuss our results in relation to inelastic neutron scattering experiments.

DOI: 10.1103/PhysRevB.65.113409

PACS number(s): 63.22.+m, 65.80.+n, 64.60.-i

The vibrational density of states (DOS) of single-wall carbon nanotubes (SWNT's) is of great interest and has been probed by heat capacity<sup>1</sup> and inelastic neutron scattering.<sup>2,3</sup> Theory predicts either one-dimensional (1D), 3D, or intermediate effective dimensionalities at very low energy,<sup>4</sup> depending on the magnitude of the intertube coupling. Here we extend heat capacity measurements down to the mK range in order to provide new information on the low-energy ( $E < 2$  meV) vibrational DOS. However, in our experiment we meet a well-known property of SWNT's (Ref. 5) to attract gases into the interstitial channels, possibly also into their inner cavities. Although this phenomenon is of great importance by itself, here we have been more focused on the problem of intrinsic vibrational states.

Sample preparation is described in Ref. 1. It consists of bundles (or "ropes") of SWNT's of an average number of  $(40 \pm 10)$  tubes, prepared by laser ablation with Ni and Co catalysts, with a residual amount up to 2% in final samples.

In order to minimize gas contamination, the sample was inserted in our usual sample holder for specific heat ( $C_p$ ) measurements under a controlled nitrogen atmosphere in a glovebox. There, the sample in the form of several foils about 1 cm<sup>2</sup> area, total mass 45 mg, once removed from an evacuated glass ampoule, was embedded in a small amount of Apiezon-N grease (30 mg) in order to improve thermal contact at very low  $T$  and to protect it from air and water contamination during transfer from the glovebox to the cryostat. We used a standard sample holder where the foils were pressed between two Si slices, the clamping being ensured by nylon screws.<sup>6</sup> The heater and thermometer were placed on opposite Si slices.  $C_p$  data were obtained by a transient heat pulse technique at each temperature point.<sup>7</sup> The heat capacity of the addenda was measured in separate experiments.

Once the sample was in the cryostat, we performed several runs over a period of 3 months, with no more exposure to air. Due to possible strong adsorption of any kind of gas [air, i.e.,  $\text{N}_2/\text{O}_2/\text{water}$ ,<sup>8</sup>  $^4\text{He}$  (Ref. 5), . . .], we have to carefully specify the experimental procedure. First, the sample

chamber, i.e., the whole calorimeter including the dilution circuit, was pumped under a primary vacuum down to  $2.5 \times 10^{-2}$  mbar at 300 K. It was necessary to introduce  $^4\text{He}$  as exchange gas in the calorimeter to enable cooling of the dilution setup down to 4.2 K. This was introduced either at 300 K or 77 K, under a pressure of  $6-7 \times 10^{-2}$  mbar at  $T = 77$  K. Once the thermal sink reached 4.2 K, we outgassed  $^4\text{He}$  by reheating the sample under dynamic secondary vacuum by successive steps up to 25–30 K; during this stage, the pressure can increase up to  $5 \times 10^{-5}$  mbar. We verified that outgassing was complete by measuring at each step the progressive decrease of  $C_p$  at, say, 8 K and its final stabilization. Indeed this temperature of outgassing (30 K) is sufficient in the case of C nanotubes, as previously shown,<sup>1,5</sup> and also in the case of He adsorption on graphite (of "Grafoil" type) if the adatoms do not form a complete monolayer, which is the case here (see discussion below). Then, the sample was let to cool down to 4.2 K under active secondary vacuum (around  $1.5 \times 10^{-6}$  mbar). This was the process for the first run A.

In order to test the role of adsorbed  $^4\text{He}$  on the heat capacity of the nanotubes, we therefore introduced the same usual amount of exchange gas at  $T \approx 8$  K, *without any more pumping*. We verified that all the gas was adsorbed by the sample, as the final vacuum reaches the usual limit of  $\approx 1.5 \times 10^{-6}$  mbar. Then data of run B were collected.

After these runs the cryostat was let to reheat to 300 K, the  $^4\text{He}$  gas pumped out to a pressure  $\approx 0.1$  mbar, and the sample kept at 300 K in these conditions for 1 month. Then, we started a new run C after pumping down to a secondary vacuum, i.e., to a pressure of  $2 \times 10^{-5}$  mbar for 4.5 days at 300 K, in order to remove possible air and water trapped by the sample during its initial transfer from controlled  $\text{N}_2$  atmosphere to the cryostat. Again, we cooled down to 4.2 K by introducing the same  $^4\text{He}$  amount at  $T = 77$  K, and, thereafter, outgassed by the same procedure as above for run A. Then data of run C were collected. In addition, we verified in this run the negligible influence ( $\leq 10\%$ ) on the heat capacity by the fact that  $^4\text{He}$  was introduced either at 300 or 77 K (with the same amount, i.e., at a pressure of  $6-7 \times 10^{-2}$  mbar at 77 K).

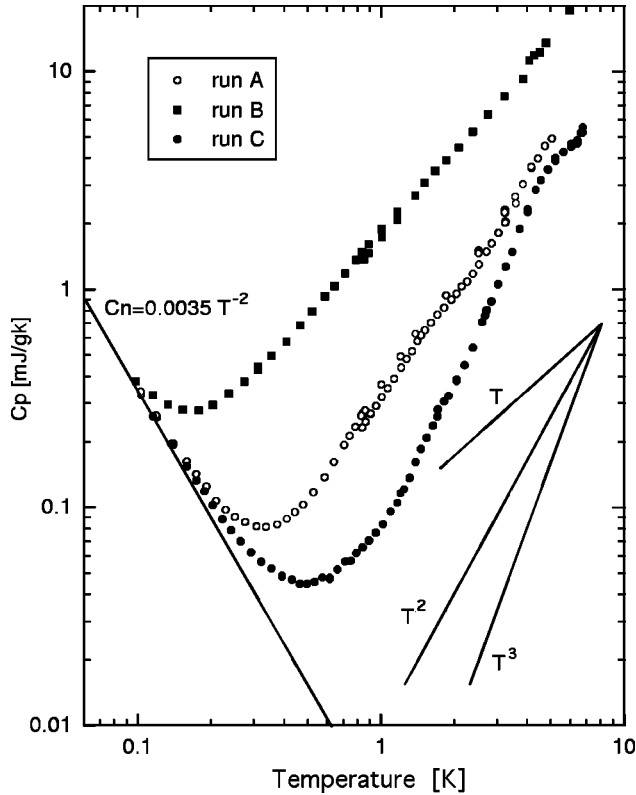


FIG. 1. Measured specific heat in a log-log plot of the SWNT sample for runs A, B, and C described in the text. The role of  $^4\text{He}$  adsorption is maximal in run B and minimal in run C. Power-law straight lines are illustrative only. All three runs yield the same nuclear hyperfine contribution  $C_n$ .

Figure 1 shows the addenda-corrected data for the three runs described above. In each,  $C_p$  decreases smoothly from  $\sim 6$  K, goes through a minimum, and then increases to reach a common 0.1 K limit. The data of our run C (best outgassing conditions) are in good agreement with Hone *et al.*<sup>1</sup> at their lower limit of 2 K. On the other hand, we find a strongly superlinear increase from 2 to 4–5 K while the data of Hone *et al.*<sup>1</sup> are nearly linear in this interval. Finally, there appears to be a break in the slope at  $\sim 4.5$  K to more nearly linear behavior.

Fits for the three runs are shown in Fig. 2 as solid lines. The negative exponent term is a nuclear hyperfine contribution originating from residual ferromagnetic catalyst particles, common for all three runs (Fig. 1). The fitted amplitude ( $C_{\text{nuc}} = 0.0035T^{-2}$  mJ/gK) corresponds to 0.7–1.0 at. % Co, in agreement with the sample analysis.<sup>1</sup> It is well documented that, except the unique  $C_{\text{nuc}}$  term, the specific heat drops monotonously with the degree of outgassing (B–A–C). After subtracting this extrinsic  $T^{-2}$  term, the remainder can be fit by  $C_p - C_{\text{nuc}} = 1.76T^{1.30}$  mJ/gK (run B),  $C_p - C_{\text{nuc}} = 0.07T + 0.24T^{1.85}$  mJ/gK (run A), both for the entire 0.1–6 K range, and  $C_p - C_{\text{nuc}} = 0.043T^{0.62} + 0.035T^3$  mJ/gK (run C) over the range 0.1–4.5 K. The process leading to the fit for run C is shown in Fig. 3.

Despite the evident influence of the adsorbed gases, in run C we have succeeded by successive outgassing in our goal of learning more about the 3D lattice regime. Subtraction of the

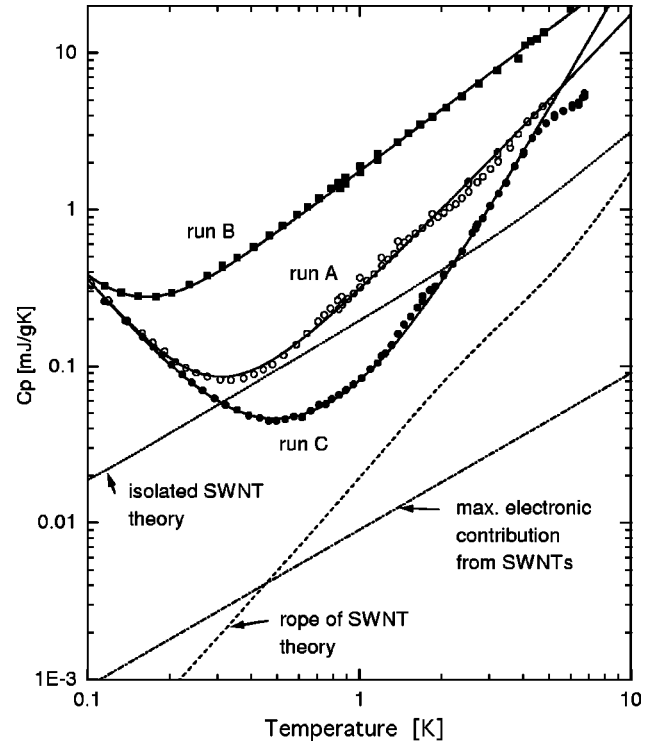


FIG. 2. Fits to the data of Fig. 1 (solid curves; see text). Also shown are theoretical behaviors for vibrational contribution of isolated SWNT's (linear below 4 K), a bundle of strongly coupled SWNT's (quadratic below 4 K) (Ref. 1), and the estimated electronic contribution if *all* the tubes were metallic.

unanticipated, but well-defined hyperfine contribution and residual power-law contributions (which we discuss latter) allows us to follow the coupled-tube regime of 3D  $T^3$  behavior over nearly four decades in  $C_p$  (Fig. 3) from 0.3 to 4.5 K. The crossover to a weaker power law above 4.5 K is quite evident, suggesting a change in effective dimensionality. In Ref. 1 this is built into the fitting model as the temperature at which the acoustic intertube modes are exhausted. These modes are represented as a Debye term with  $\theta_D^\perp$  a direct measure of the intertube coupling strength.<sup>1</sup>

$C_p(T)$  may be calculated from the density of vibrational modes  $D(E)$ , where  $E$  is the phonon energy. Inelastic neutron scattering measures a generalized vibrational density of states, (GDOS) closely related but not identical to  $D(E)$ .<sup>2</sup> In practice,  $C_p$  is rather insensitive to weak features in  $D(E)$  since a weighted integral is involved. This intrinsic “smearing” of distinct features will be even more severe in real samples containing a distribution of tube diameters. The GDOS measured on different SWNT samples<sup>2,3</sup> and in various conditions consistently demonstrates a change of slope versus energy between 1.5 and 2 meV. Data obtained on a sample of the same origin as ours are shown in Fig. 4, with a crossover at 1.6 meV. Although we hope that some ambiguities about their temperature dependence and exact limit  $E \rightarrow 0$  behavior will be clarified in the future by new neutron experiments,<sup>9</sup> we can say here that they all show consistency with the change in the  $C_p(T)$  regime we report here at 4.5 K (which corresponds within the dominant phonon approxima-

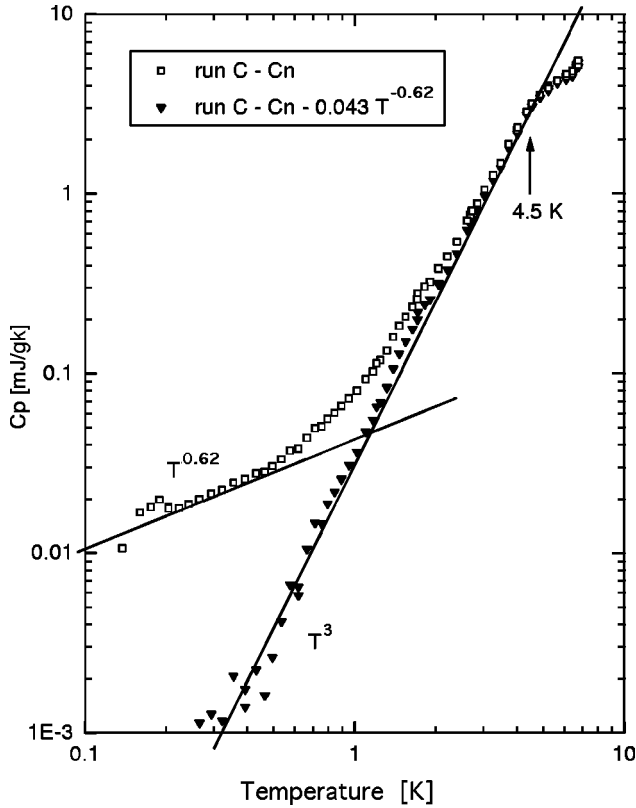


FIG. 3. After subtraction of the nuclear term in run C, the data can be fit with  $0.043T^{0.62} + 0.035T^3$  mJ/gK. The vibrational  $T^3$  term is well defined from 0.3 to 4.5 K.

tion to an energy of 1.7 meV). They also suggest that  $G(E)$  extrapolates to zero at  $E=0$ , rather than at finite values as expected for isolated tubes.<sup>1,2</sup>

Concerning the vibrational contribution, we conclude that the two  $C_p$  experiments are in overall agreement. The present data give a better estimate of the intertube coupling energy, 1.7 vs. 1.2 meV in Ref. 1, by extending the data to lower  $T$ . A linear contribution to  $C_p(T)$ , associated with LA modes propagating along decoupled tubes expected at higher  $T$ , is not observed directly but may be deduced from curve fitting *only* if the data extend well above the crossover temperature.<sup>1</sup> Such a difference in the coupling energy can be accounted for by differences in intertube interactions in ropes of different samples, due to differences in chirality or diameters of neighboring tubes.

Finally, such behavior is reminiscent of other quasi-1D compounds: for instance, 1D conductors in the Peierls state, where a dimensionality crossover for the phonons occurs in the  $T$  range of a few K, between a low- $T$  3D regime due to the interactions between adjacent chains to a more quasi-1D regime characterized by  $C_p \propto T^{2.5} - T^{2.8}$  at higher  $T$ .<sup>10</sup> This can be described by a strong anisotropy of the force constants between and along the chains.<sup>11</sup>

A second property to be briefly discussed in this paper is the power-law terms and their relation to adsorbed  $^4\text{He}$ . The linear (run A) and sublinear ( $\sim T^{0.62}$ , run C), contributions are of similar amplitude below 1 K and much larger than the estimated maximum electronic contribution of the nanotubes

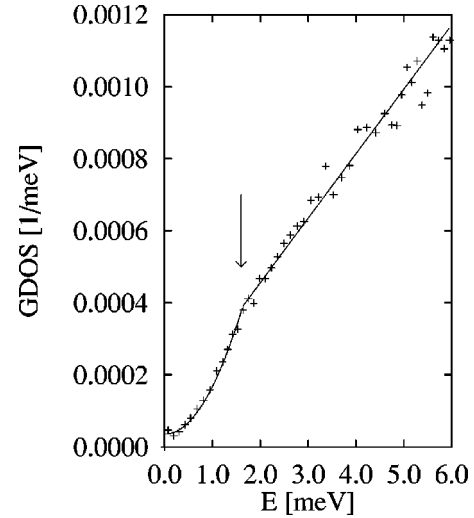


FIG. 4. Demonstration of the change of slope of GDOS at 1.6 meV measured by inelastic neutron scattering at 100 K on the sample of the same origin (taken from Ref. 3). These data suggest almost  $E^2$  behavior up to 1.6 meV (in agreement with  $C_p \sim T^3$ ); however, a detailed study of different samples and in various controlled experimental conditions will be given in Ref. 9 (the solid line is only a guide for the eye).

(see Fig. 2). Also, they are too large for the Ni impurity contribution. This term is reminiscent of low-energy excitations contributions to  $C_p$  in disordered systems, but again with unusually large amplitude. It can be compared with the case of porous materials like silica aerogels with comparable amplitudes at 1 K, which in addition show a dramatic increase due to adsorbed He.<sup>12</sup>

Our results are probably the first to demonstrate the effect of He in a 1D system as nanotubes in low- $T$   $C_p$ , which is certainly not of only academic interest, and it deserves a well-controlled experimental investigation. Here we can only roughly discuss the progressive evolution of the vibrational contribution from  $T^{1.85}$  (run A) to  $T^{1.30}$  (run B). In this latter case,  $C_p - C_{\text{nuc}}$  is well represented by only a  $T^{1.30}$  contribution, within 10% between 0.15 K and 6 K, without any indication of a phase transition or distinct change of regime. As this contribution is mainly the effect of adsorbed  $^4\text{He}$ , we can discuss this result in the framework of the few proposed models for the properties of  $^4\text{He}$  in C nanotubes.

But first, we can compare it to the case of adsorption on graphite (“Grafoil” type), topologically similar to the 2D surfaces of SWNT’s.<sup>13,14</sup> The absence of a sharp maximum in  $C_p$  in the  $T$  range 2–6 K indicates that the adatoms do not form a complete monolayer on the 2D carbon lattice. Indeed, taking into account the estimated huge specific surface of C nanotubes—300 m<sup>2</sup>/g in comparison to 20–30 m<sup>2</sup>/g for Grafoil—and the concentration of  $^4\text{He}$  introduced in the calorimeter ( $\approx 7 \times 10^{19}$  atoms), we estimate that the maximum density of adatoms is  $\approx 2$  atoms/nm<sup>2</sup>, far below the first monolayer completion in graphite reached for  $n_1 = 11.5$  atoms/nm<sup>2</sup> at  $T=1$  K.<sup>13</sup> Indeed, from both the absence of any pronounced maximum in our whole  $T$  range and the amplitude of the  $T^{1.3}$  contribution, one could conclude a very low effective coverage, probably less than 1.5 or

2 atoms/nm<sup>2</sup>, always in comparison to data in Grafoil (from Greywall<sup>15</sup>). In these conditions, inhomogeneities of the substrate probably dominate the adsorption (as in Grafoil), because <sup>4</sup>He is preferentially adsorbed at the most energetic sites, i.e., defective ones.

Considering now the specific geometry of bundles of SWNT's: <sup>4</sup>He adsorption experiments,<sup>5</sup> which confirm the large desorption effect up to 25 K, show that <sup>4</sup>He atoms are very strongly bound in the interstitial channels of the bundles, with a predominant 1D character. Other authors,<sup>16</sup> on the basis of a separation of 0.42 nm between localized <sup>4</sup>He sites (or a linear density of 2.4 atoms/nm) along the interstitial channels, predict the occurrence of a sharp  $C_p$  anomaly, which should occur around  $T_c \approx 0.36$  K, for a site occupancy near 1/2, as the signature of a solid lattice to gas phase transition. In addition, always supposing 1D confinement for the <sup>4</sup>He adsorption, the authors of Ref. 17 predict a quasicontinuous liquid to solid transition when the linear density increases above  $\approx 2.0$  atoms/nm. From our present estimate of <sup>4</sup>He atomic concentration (around 3% of C atoms) and supposing that our samples are organized in bundles of 37 SWNT's to form a regular hexagonal lattice close to the experimental value of  $40 \pm 10$ , which correspond to 54 interstitial channels, one obtains a mean intersite distance of 0.40 nm (or a linear density of 2.5 atoms/nm), therefore similar to a complete site occupancy. In such conditions,

a specific heat anomaly would be observed in the framework of Ref. 16. Once more, the absence of any transition probably implies that most of the <sup>4</sup>He atoms could be trapped outside the regular lattice of bundles, in some defective sites<sup>18</sup> such as branching of bundles, catalysts aggregates, etc.

Finally, after this detailed analysis of He adsorption, we make again a note on the comparison of our data of run C from 2 to 4–5 K with the data and theoretical models of Ref. 1. We might consider that they are in a fair agreement especially if we estimate possible effects due to the difference in the samples masses, which yield huge differences in corresponding surfaces and their sensitivity to gas adsorption.

In summary, we have investigated the heat capacity of bundles of SWNT's in the  $T$  range from 0.1 K to 7 K for different conditions of gas (essentially <sup>4</sup>He) adsorption. For the best outgassed sample, we found a vibrational  $T^3$  contribution below 4.5 K down to 0.3 K, which demonstrates the three-dimensional character of the bundles for low-frequency phonons. In the presence of <sup>4</sup>He, the vibrational contribution is still very monotonic, varying like  $T^{1.30}$ , without any sign of a phase transition for the <sup>4</sup>He “sublattice.”

Work at Penn was supported by U.S. DOE Grant No. DEFG02–98ER45701. The authors at CRTBT are grateful to H. Godfrin for discussions about the adsorption on graphite and to J. Marcus (LEPES) for his help in preparing the experiment in a controlled N<sup>2</sup> atmosphere.

\*Electronic address: lasjau@polycnrs-gre.fr

<sup>1</sup>J. Hone, B. Batlogg, Z. Benes, A.T. Johnson, and J.E. Fischer, *Science* **289**, 1730 (2000).

<sup>2</sup>S. Rols, Z. Benes, E. Anglaret, J.L. Sauvajol, P. Papanek, J.E. Fischer, G. Goddens, H. Schober, and A.J. Dianoux, *Phys. Rev. Lett.* **85**, 5222 (2000).

<sup>3</sup>S. Rols, Ph. D. thesis, Université de Montpellier II, 2000; Z. Benès, Ph. D. thesis, University of Pennsylvania, 2001.

<sup>4</sup>L.X. Benedict, S.G. Louie, and M.L. Cohen, *Solid State Commun.* **100**, 177 (1996).

<sup>5</sup>W. Teizier, R.B. Hallock, E. Dujardin, and T.W. Ebbesen, *Phys. Rev. Lett.* **82**, 5305 (1999).

<sup>6</sup>J.C. Lasjaunias and P. Monceau, *Solid State Commun.* **41**, 911 (1982).

<sup>7</sup>F. Zougmore, J.C. Lasjaunias, and O. Béthoux, *J. Phys. (Paris)* **50**, 1241 (1989).

<sup>8</sup>Y. Maniwa, Y. Kumazawa, Y. Saito, H. Tou, H. Kataura, H. Ishii, S. Suzuki, Y. Achiba, A. Fujiwara, and H. Suematsu, *Jpn. J.*

*Appl. Phys., Part 2* **38**, L668 (1999).

<sup>9</sup>J. L. Sauvajol (private communication).

<sup>10</sup>Y. Hongshun, J.C. Lasjaunias, and P. Monceau, *J. Phys.: Condens. Matter* **11**, 5083 (1999).

<sup>11</sup>S.M. Genensky and G.F. Newell, *J. Chem. Phys.* **26**, 486 (1957).

<sup>12</sup>R. Calemczuk, A.M. de Goer, B. Salce, R. Maynard, and A. Zarembovitch, *Europhys. Lett.* **3**, 1205 (1987).

<sup>13</sup>M. Bretz, J.G. Dash, D.C. Hickernell, E.O. McLean, and O.E. Vilches, *Phys. Rev. A* **8**, 1589 (1973).

<sup>14</sup>R.L. Elgin and D.L. Goodstein, *Phys. Rev. A* **9**, 2657 (1974).

<sup>15</sup>D.S. Greywall, *Phys. Rev. B* **47**, 309 (1993).

<sup>16</sup>M.W. Cole, V.H. Crespi, G. Stan, C. Ebner, J.M. Hartman, S. Moroni, and M. Boninsegni, *Phys. Rev. Lett.* **84**, 3883 (2000).

<sup>17</sup>M. Boninsegni and S. Morini, *J. Low Temp. Phys.* **118**, 1 (2000).

<sup>18</sup>A. Thess, R. Lee, P. Nikolaev, H. Dai, P. Petit, J. Robert, C. Xu, Y.H. Lee, S.G. Kim, A.G. Rinzler, D.T. Colbert, G.E. Scuseria, D. Tománek, J.E. Fischer, and R.E. Smalley, *Science* **273**, 483 (1996).